J Electr Eng Technol.2015; 10(4): 1626-1634
http://dx.doi.org/10.5370/JEET.2015.10.4.1626

ISSN(Print) 1975-0102
ISSN(Online) 2093-7423

Optimization of Parameters for LCL Filter of Least Square Method Based Three-phase PWM Converter

Hong Zheng†, Zheng-feng Liang*, Meng-shu Li* and Kai Li*

Abstract – LCL filters are widely used in three-phase PWM converter for its advantages of small volume, low cost and inhibition of high frequency current harmonic. However, it is difficult to optimize its design because its parameters are mutually influenced while the value of each parameter for LCL filter has impacts on the converter's cost and size. In this paper, the target of optimization is to minimize the parameter values of LCL filter, and an optimization method for parameters of LCL filter of three-phase PWM converter based on least square method is proposed. With this method, a quantitative calculation of the harmonic component of the converter's side phase voltage is performed first, and then the quantitative relationship between phase voltage harmonics and grid phase current harmonics is analyzed. After that, the attenuation requirement of each harmonic is obtained by taking into account the requirements for each harmonic component of grid current. Then according to the optimization objective, the objective function with minimum harmonic attenuation deviation is established, and least squares method is adopted for three-dimensional global searching of parameters for LCL filter. Thus, the designed harmonic attenuation curve approximates the minimum attenuation requirements, and the optimized LCL filter parameters are obtained. Finally, the effectiveness of the method is verified by the experiments.

Keywords: LCL filter, Three-phase PWM converter, Least squares method, Parameter optimization, Harmonic attenuation curve

1. Introduction

Because three-phase voltage-type PWM converter has the advantage of high power factor, good dynamic response, and bidirectional power flowing, etc. it is widely used in grid-connected power generation, motor drive, control of battery charge and discharge and other fields [1-4]. Meanwhile, the three-phase PWM converter with pulse width modulation (PWM) generates high frequency switching harmonics, so it requires high-frequency filter in its AC side. Compared to the traditional L and LC type filter, LCL filter enjoys the advantages of small size, low cost, and high attenuation effect on high-frequency current harmonic and so on, and thus it is more suitable for high-power applications. However, LCL filter has three parameters. Moreover, the parameters have a high degree of coupling and the mutual effects between them are difficult to analyze, and due to some other reasons, it is hard to design the parameters.

In recent years, scholars have done a great research work on the design and optimization of LCL filter parameters. In the parameter design, Marco Liserre has done a detailed theoretical analysis on the steps and constraints of parameters design for LCL filter [5-6], and established a complete design approach for the first time. Based on that, the literature [7-9] got the containing range for the three parameters of LCL filter by studying the relationship between the changes of the filter's each parameters and ripple rejection and resonant frequency, and then the appropriate parameters were determined after several attempts and repeated verifications, but the obtained LCL filter parameters are not optimal. In optimizing the filter parameters, the literature [10] considered the voltage harmonics generated by SVPWM method. Meanwhile, with maximum single harmonic attenuation of grid current as the optimization objective, the method for designing optimal LCL parameters by doing iterative computation based on harmonic voltage value was proposed in literature [10]. However, in the optimization process, the resonant frequency and inductance scale factor were known input, thus reducing the number of constraints, therefore, only a simple one-dimensional local search was performed. Based on literature [10], literature [11] took the minimum of total harmonic distortion (THD) as the target for optimization. Then, a THD estimation model was established through analysis and calculation of harmonic current value, and a more simplified gradient algorithm with multiple starting point was realized for LCL filter parameter optimization. However, the resonance frequency was a known input in the optimization process, thus reducing the constraints, and only a two-dimensional local search was done. In literature

† Corresponding Author: Dept. of Automation, University of Electronic Sci&Tech of China, China. (macrozheng@uestc.edu.cn)
* Dept. of Automation, University of Electronic Sci&Tech of China, China. (lzhf0228@163.com, 378617447@qq.com, 2207301022@uestc.edu.cn)
Received: December 4, 2014; Accepted: March 29, 2015

[12], in accordance with the requirements of filtering performance, a LCL filter parameter optimization method was proposed that the total amount of inductance was minimized, but in the design process, the power factor and the value ratio between harmonic current and voltage harmonic of the switching frequency were known and thus it is a one-dimensional local search method.

In this paper, an optimization method for parameters of LCL filter of least square method based three-phase PWM converter is proposed. First, through the analysis of working principle and characteristics of converter SVPWM modulation, peaks of each harmonic for side phase voltage of converter is quantitatively calculated based on Fourier series expansion method. Secondly, the quantitative relationship between phase voltage harmonics and grid-connected phase current harmonics is analyzed, and minimum requirements for the filter attenuation rate is obtained combining with requirements for each harmonic of grid currents. Thirdly, with the optimization target of minimizing the parameter values of LCL filter, the objective function with minimum harmonic attenuation deviation is established, and least squares method is adopted for three-dimensional global searching of parameters for LCL filter, so that the actual attenuation curve is approaching the required minimum attenuation rate, resulting in optimized parameters value. Finally, the experimental platform is established and the validity of the method is verified.

2. Calculation of PWM Voltage Harmonic

For better clarifying the design method proposed in this paper, three-level converter is taken as the research object. The main circuit of three-phase three-level voltage source converter is shown in Fig. 1, where u_{gx} $(x=a,\ b,\ c)$ represents each grid phase voltage, and u_x refers to output phase voltage of converter at the AC side, and S_{x1}, S_{x2}, S_{x3} and S_{x4} are the four switches on the bridge arm corresponding to x, and L is filter inductance of the converter bridge side, and L_g refers to filter inductance of grid-side, and C_f is the filter capacitor, and R_d is the damping resistor.

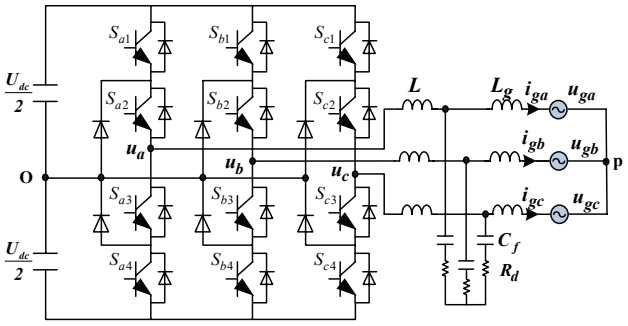

Fig. 1. Main circuit of the three-phase three-level grid-connected VSR with a LCL filter

2.1 Analysis of SVPWM

Three-level SVPWM has 27 voltage vectors which is composed of 3 zero vectors, 12 short vectors, 6 medium vectors and 6 long vectors. As shown in Fig. 2.

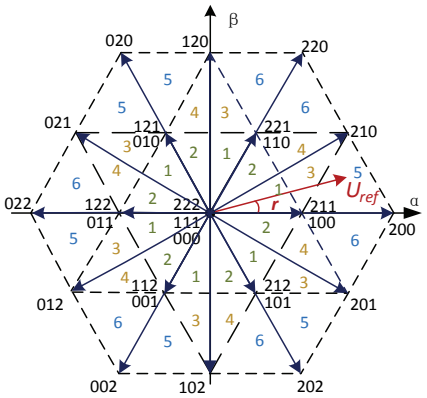

Fig. 2. Voltage space vectors of SVPWM

Here, U_{ref} refers to reference voltage vector, and r is the rotation angle of the reference voltage vector.

$$S_x=\begin{cases}2,\left(S_{x1},S_{x2},S_{x3},S_{x4}\right)=\left(1,1,0,0\right)\\1,\left(S_{x1},S_{x2},S_{x3},S_{x4}\right)=\left(0,1,1,0\right)\\0,\left(S_{x1},S_{x2},S_{x3},S_{x4}\right)=\left(0,0,1,1\right)\end{cases}\tag{1}$$

In this paper, the three-level SVPWM method of literature [14] is adopted. Take U_{ref} in Fig. 2 as an example, which locates at the small section 5 of the big section I. Its small vectors are selected as 100 and 211, which is defined as $U_1=U_{dc}/3$, and the action time is T_1. Meanwhile, its medium vector is selected as 200, defined as $U_2=U_{dc}/2\times e^{j\pi/6}$, and the action time is T_2. And its long vectors are selected as 210, defined as $U_3=2U_{dc}/3$, and the action time is T_3. Then, the relationship among them is described in the following formula (2).

$$U_{ref}T_s=U_1T_1+U_2T_2+U_3T_3\tag{2}$$

Here, T_s is the switching period, and $T_1+T_2+T_3=T_s$. Meanwhile, by formula (2), the value of T_1, T_2 and T_3 can be obtained, as shown in formula (3).

$$\begin{cases}T_1=2T_s[1-m_u\sin(\pi/3+r)]\\T_2=T_s[2m_u\sin(\pi/3-r)-1]\\T_3=2T_sm_u\sin(r)\end{cases}\tag{3}$$

where the modulation ratio is $m_u=\sqrt{3}U_{ref}/U_{dc}$, and the range of values for m_u is $0\le m_u\le 1$, and U_d, and the range of values for m_u is $0\le m_u\le 1$, and U_{dc} is the DC link voltage. Moreover, take phase a as an example, the voltage waveform of voltage u_{ao} with phase a relative to the capacitor neutral point o is analyzed. For the voltage u_{ao}

in a switching cycle T_s, (1) when $S_x=1$, it is 0 ; (2) when $S_x=2$, it is $+u_{dc}/2$, with a positive level duty cycle $d_{u(k)}^{+}(0\le d_{u(k)}^{+}\le 1)$; (3) when $S_x=0$, it is $-u_{dc}/2$ with a negative level duty cycle $d_{u(k)}^{-}(-1\le d_{u(k)}^{-}\le 0)$. Therefore, the duty cycle of U_{ref} in Fig. 2 can be represented by formula (4).

$$d_u^+=\frac{T_s-T_1/2}{T_s}=m_u\sin(\pi/3+r) \tag{4}$$

According to the switch vector sequence [14], the duty cycle d_u in each section of Fig. 2 are shown in Appendix Table 1.

For the digital implementation of SVPWM, the rotation angle r of the voltage vector U_{ref} steps once per switching period. And the step angle is $d_r=360°/m_f$ where $m_f=f_{sw}/f_g$ is the carrier ratio, and f_{sw} is the switching frequency, and f_g is the grid frequency. Take $-180°$ as the moment of 0 and $+180°$ as T, and then spread u_{ao} in a grid period.

As shown in Fig. 3, separate the switching period T_s into m_f intervals, where in the length of interval 1 and interval m_f+1 is $T_s/2$ while other intervals is T_s. Meanwhile, the rotation angle corresponding to interval k is $r_k=(k-1)\times 360°/m_f$.

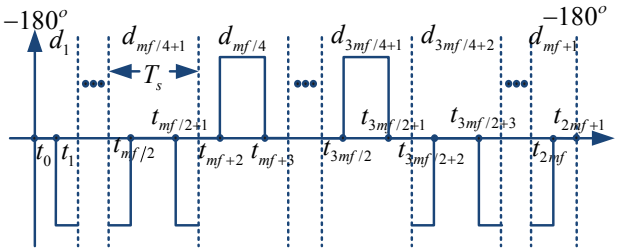

Fig. 3. One period spread waveforms of u_{ao}

To facilitate the unified computing, the zero level of u_{ao} is regarded as positive level duty time when u_{ao} outputs negative voltage pulse. Provided that $d_{u(k)}^{+}$ is the positive level duty cycle of interval k and t_k is the transition time of voltage pulse k^{th}, the transition time of each voltage pulse can be obtained by formula (5).

$$\begin{cases} t_0=0, \quad t_{2m_f+1}=T \\ t_1=d_{u(1)}^{+}/2T_s \\ t_{2k-2}=t_{2k-3}+(\dfrac{2-d_{u(k-1)}^{+}+d_{u(k)}^{+}}{2})T_s \\ \qquad (k=2,3,...,m_f+1) \end{cases} \tag{5}$$

2.2 Calculation of voltage harmonic

For the voltage u_{ao} is a periodic function, the values of each harmonic can be calculated based on the principle of Fourier series expansion method, as shown in formula (6).

$$u_{ao}(t)=a_o+\sum_{h=1}^{\infty}[a_h\cos(h\omega_1 t)+b_h\sin(h\omega_1 t)] \tag{6}$$

where $\omega_1=2\pi f_g$ is the grid angular frequency; a_0 is the DC component and h is the harmonic number.

According to the transition time t_0, t_1, ... t_{2mf+1}, and substitute u_{ao} into integral formulas (6), the calculation of each voltage harmonic can be derived, as shown in formula (7) - (9).

$$a_h=\frac{U_{dc}}{2h\pi}[\sum_{k=1}^{m_f+1}\sin(h\omega_1 t_{2k-1})-\sum_{k=1}^{m_f}\sin(h\omega_1 t_{2k}) -2\cos(\frac{h\omega_1 T_s}{2})] \tag{7}$$

$$b_h=\frac{U_{dc}}{2h\pi}[\sum_{k=1}^{m_f}\sin(h\omega_1 t_{2k})-\sum_{k=1}^{m_f+1}\sin(h\omega_1 t_{2k-1}) +2\sin(\frac{h\omega_1 T_s}{2})] \tag{8}$$

$$c_h=\sqrt{a_h^2+b_h^2}\ . \tag{9}$$

For phase a, the relationship of u_{ao}, u_{ap} and u_{po} is represented as $u_{ao}=u_{ap}+u_{po}$, where u_{po} is the voltage of the load capacitance midpoint p relative to midpoint o of DC capacitor and $u_{po}=(u_{ao}+u_{bo}+u_{co})/3$. In terms of the relationship among each harmonic component of u_{ao}, u_{ap} and u_{po} [16], it can be known that the components of output phase voltage u_{ap} are composed of the fundamental wave and the rest components of u_{ao} excluded of carrier frequency multiplication and third sideband harmonics. Therefore, the values of u_{aph} at the h-order of voltage u_{ap} can be gained by formula (10).

$$U_{aph}=\begin{cases} c_h, \ h=1 \ or \ n+m\times m_f \\ \quad (m=1,2,3... \text{ and } n=\pm1,\pm2,\pm5,...) \\ 0, \ h=n+m\times m_f \\ \quad (m=1,2,3... \text{ and } n=0,\pm3,\pm6,...) \end{cases} \tag{10}$$

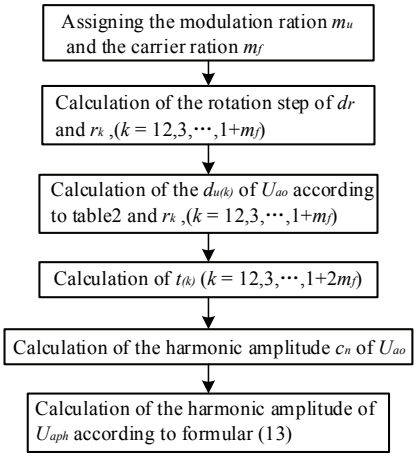

Fig. 4. Flow chart of the harmonic calculation of phase voltage

where n is the fundamental doubling harmonic and m is the carrier doubling harmonics.

Based on the above analysis, the calculation process of voltage harmonic U_{aph} for side output phase of converter based on three-level VSC with SVPWM can be obtained, as shown in Fig. 4.

With the calculation process shown in Fig. 4, each harmonic component of U_{aph} can be obtained.

3. Optimization of Filter Parameters

3.1 Equivalent model of filter

Assuming that the converter keeps three-phase equilibrium, and parameters of each phase are consistent, and the voltage source for the grid is ideal, then single-phase equivalent model of fundamental component and harmonic component based on the LCL filter are shown in Fig. 5(a) and Fig. 5(b), respectively.

In addition, the fundamental component of the output phase voltage at the AC side of converter is defined as $u_{ap1}(t)=|U_{ap1}|\times\cos(\omega_1 t+\theta)$ and the fundamental component of grid phase current is defined as $i_{g1}(t)=|I_{g1}|\times\cos(\omega_1 t+\beta)$ while that of the grid phase voltage is $u_g(t)=|U_g|\times\cos(\omega_1 t)$. From Fig. 5, the relationship among fundamental component u_{ap1} of output phase voltage at the AC side of the converter, the fundamental component of the grid phase current i_{g1} and the grid phase voltage u_g in the s-domain can be represented at the following formula (11).

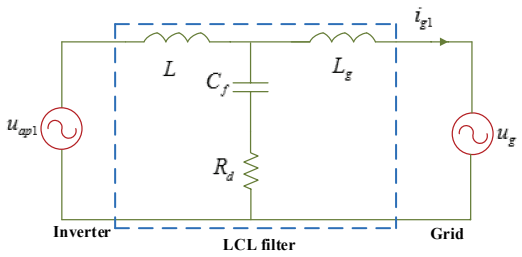

(a)

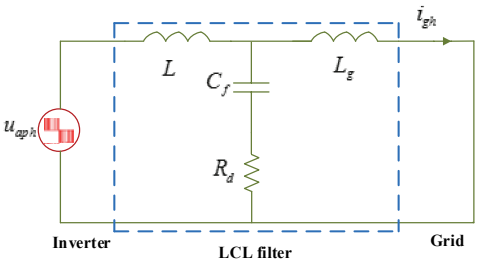

(b)

Fig. 5. Single-phase equivalent circuit of LCL filter: (a) Single-phase equivalent model of fundamental component; (b) Single-phase equivalent model of harmonic component

$$I_{g1}(s)=\frac{(sR_dC_f+1)U_{ap1}(s)-(s^2LC_f+sR_dC_f+1)U_g(s)}{s^3LL_gC_f+s^2R_dC_f(L+L_g)+s(L+L_g)} \quad (11)$$

According to Fig. 5, the relationship between the h-order harmonic component U_{aph} of output phase voltage at the AC side and the h-order harmonic component I_{gh} of grid phase current in the s-domain is shown at the following formula (12).

$$\frac{I_{gh}(s)}{U_{aph}(s)}=\frac{(sR_fC+1)}{s^3LL_gC_f+s^2R_dC_f(L+L_g)+s(L+L_g)} \quad (12)$$

3.2 Attenuation curve of filter

IEEE519 and IEEE1547 are two standard protocols for current harmonics of grid converter, commonly used in distributed generation and renewable energy systems, whose spectrum standard of grid current harmonic is as shown in Fig. 6.

In Fig. 6, I_{ghmax} is the maximum value for h-order grid current harmonics, and its standard value is the percentage of h-order harmonics and the fundamental components I_{g1}. Moreover, the standard also provides the number of even harmonics is 25% of that of odd harmonics.

In terms of Fig. 6, the maximum value for h-order filter output current can be obtained, and combined with the h-order harmonics U_{aph} of filter input voltage, the minimum requirements for attenuation rate G_{hReq} of h-order harmonics for the filter can be known, and their relationship is as shown in formula (13).

$$G_{hReq}=20\log\left|\frac{I_{gh\max}\times I_{g1}}{U_{aph}}\right| \quad (13)$$

From formula (13), it can be found that the calculation of actual attenuation curve for LCL filter is as shown in the following formula (14).

$$G_h=20\log\left|\frac{(sR_dC+1)}{s^3LL_gC_f+s^2R_dC_f(L+L_g)+s(L+L_g)}\right| \quad (14)$$

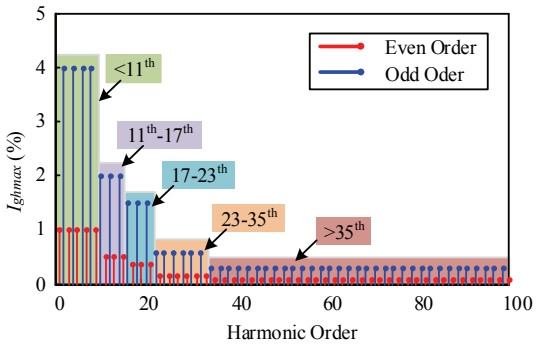

Fig. 6. Spectrum standard of grid current harmonic

where $s=jh\omega_1$ when $h=2, 3, 4\ldots$. If U_{aph}, L, L_g, C_f and R_d are known, the actual attenuation curve G_h of LCL filter can be calculated by formula (14).

3.3 Filter parameters constraints

According to the literature [5-9], the following LCL filter parameters constraints can be obtained:

1) Reactive power generated by capacitance is generally required to be no more than 5% of the system's rated power P_n, as follows:

$$C_f \le \frac{5\%P_n}{3w_1U_{ph}^2} \tag{15}$$

2) Considering the capacity of outputting active power by VSC under stable conditions, the total inductance $L_T=L+L_g$ should satisfy the formula (16):

$$L_T \le \frac{U_{dc}/\sqrt{3}-U_{phm}}{w_1 I_{phm}} \tag{16}$$

3) The resonant frequency is generally defined to be between 10 times of the fundamental frequency f_g and 0.5 times of the switching frequency f_{sw}, as shown in the following formula (17):

$$10f_g \le f_{wes} = \frac{1}{2\pi}\sqrt{\frac{L+L_g}{LL_gC_f}} \le 0.5f_{sw} \tag{17}$$

4) The design of damping resistor R_d needs to consider a compromise between the system damping and the loss of damping, and its value is generally 1/3 of capacitive reactance for filter capacitor C_f at a resonant frequency of f_{res}, as follows.

$$R_d \approx \frac{1}{6\pi f_{res}C_f} \tag{18}$$

where f_{res} is the resonant frequency of the filter, and U_{ph} is the effective value of grid phase voltage, meanwhile, U_{phm} and I_{phm} are peak values of grid phase voltages and phase currents.

3.4 Optimization of parameters based on least squares method

Least squares method is a mathematical optimization method, which finds the best matching function for a given set of data through minimizing the sum of the squares of the error. By the formula (14), it can be seen that the larger the value of the filter parameter, the smaller the value of G_h, i.e. the better the suppression effect of its current harmonics, but the greater the volume of the filter and the higher the cost at the same time. Therefore, the value of G_h can be increased as far as possible when the requirements of harmonic suppression are satisfied, in order to minimize the filter parameters. In this paper, the least squares method is applied to the optimization of filter parameters. With the goal of minimizing the parameters of LCL filter, and in terms of the constraints on filter parameters obtained by the formula (15) - (18), a three-dimensional global search for L, L_g and C_f is performed, so that the actual attenuation curve constantly approaches the required minimum attenuation rate, and then the optimized filter parameters are found.

Considering that some margin is required in the practical application of the filter, M can be defined as the margin value of the filter attenuation curve, which ranges from 0 to 1. Meanwhile, the actual attenuation rate G_h of each harmonic and the required minimum attenuation rate G_{hReq} should satisfy the formula (19).

$$G_h \le G_{h\mathrm{Re}q}/M \tag{19}$$

The sum of deviation between actual attenuation rate G_h of each harmonic and the minimum requirements of attenuation rate G_{hReq} can be calculated by formula (20).

$$G_{Err} = \sum_{h=2}^{\infty}(G_h - M\times G_{hReq})^2 \tag{20}$$

In summary, the interrelationships of each part of the optimization design above is shown in Fig.7.

Besides, the program flow chart of the filter parameters design is shown in Fig. 8 and the design steps of the method for LCL filter parameters optimization proposed in the paper are as follows, where L^*, L_g^*, C_f^* and R_d^* are the optimal values of the filter parameters.

Step 1: The system's rated power P_n, the switching frequency f_{sw}, the DC bus voltage U_{dc}, grid phase voltage U_{ph} and frequency f_g are known, and then the ranges of filter parameter constraints are calculated as $0<L<L_{Tmax}$,

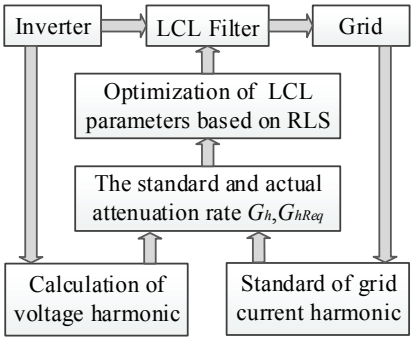

Fig. 7. Interrelationship of each part of the optimization design method

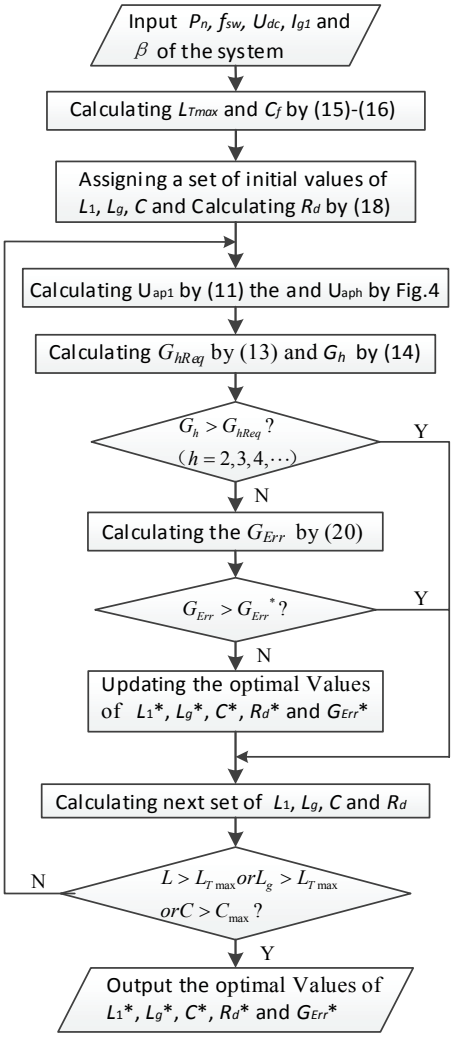

Fig. 8. Flow chart of the LCL filter parameters design

$0<L_g<L_{Tmax}$ and $0<C_f<C_{fmax}$ according to formula (15) - (17);

Step 2: given a set of L, L_g and C_f within the range got in Step 1, then if the parameters are successfully defined, use formula (18) to calculate the damping resistor R_d and go to step 3, otherwise go to step 8;

Step 3: the current peak value $|I_{g1}|$ and power factor angle β are known, and thus the peak value and phase angle of the converter output phase voltage at the AC side can be obtained by formula (11);

Step 4: the modulation ratio m_u can be obtained by the peak value of the output phase voltage, and then U_{aph} can be obtained by Fig. 5 for peak value of each harmonic of phase voltage;

Step 5: the maximum value I_{ghmax} of peak value for each harmonic of grid current can be obtained from Fig. 7, and then the required minimum attenuation rate G_{hReq} can be calculated by the formula (13) ;

Step 6: given the margin value of filter attenuation curves as M, then the actual attenuation curve of LCL filter can be obtained by substituting L, L_g, C_f and R_d into formula (14), and it can be seen whether it satisfies formula (19), so return to step 2 if not satisfied, otherwise go to step 5;

Step 7: calculate by formula (20) and determine whether it satisfies $G_{Err}<G_{Err}^*$, and if it satisfies, then update the value of optimal filter parameters as $G_{Err}^*=G_{Err}$, $L^*=L$, $L_g^*=L_g$, $C_f^*=C_f$ and $R_d^*=C_d$ while back to step 2;

Step 8: stop searching, and output the values of optimal filter parameters as $L^*=L$, $L_g^*=L_g$, $C_f^*=C_f$ and $R_d^*=C_d$

3.5 A practical design example

The design parameters of system are as follows: rated power P_n is 10 kVA, and DC voltage U_{dc} is 700 V, and the percentage between effective value of grid phase voltage U_{ph} and frequency f_g are 220V/50Hz, and the switching frequency f_{sw} is 9kHz.

The peak value of fundamental wave for phase voltage U_{g1} and modulation ratio m_u is 1when the power factor of the converter, and the peak value of grid current I_{g1} is 21A, and the phase β is zero. To verify the effects of the design method in extreme cases, the margin value M of filter attenuation curve is 1.

The filter parameters constraints can be obtained by (15)-(16): C_{max}=14uF and LT_{max}=10mH. Then, the three-dimensional searching scope can be 0.1mH$\leqslant L\leqslant$10mH, 0.1mH$\leqslant L_g\leqslant$10mH and 0.2uF$\leqslant C_f\leqslant$10uF. Given the value of capacity C_f and searching L and L_g, a set of values of L and L can be obtained while the sum of harmonic deviation G_{Err} is minimal. And by repeating the same searching process, the parameters of L, L_g, and G_{Err} with various C_f are shown in Fig. 9.

In Fig. 9, it can be found that the parameters of G_{Err}, L and $L+L_g$ converge to the minimum point while C_f is 3.1uF, which have been marked in the figure. Therefore, the values of L, L_g and C_f at the minimum point, as shown in Table 1, are the optimal parameters obtained by the proposed method.

The traditional method proposed in literature [5] and the new proposed method are respectively adopted to design LCL filter parameters, as it shown in Table 1.

From Table 1, it can be clearly seen that the parameters

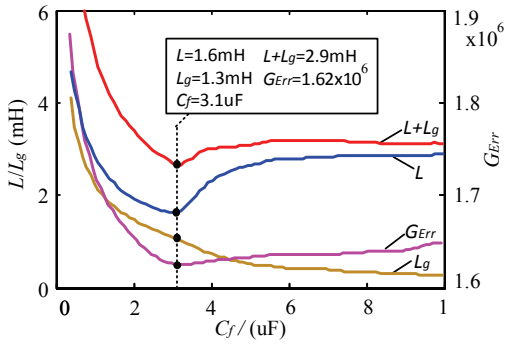

Fig. 9. Values of L and L_g and the minimal values of G_{Err} with various values of C_f

Table 1. LCL filter parameters before & after optimization

Filter parameter	L /mH	L_g /mH	C_f/uF	R_d /Ω	f_{res}/Hz
Traditional method	4	2	6	5	1780
New method	1.6	1.3	3.1	5	3376

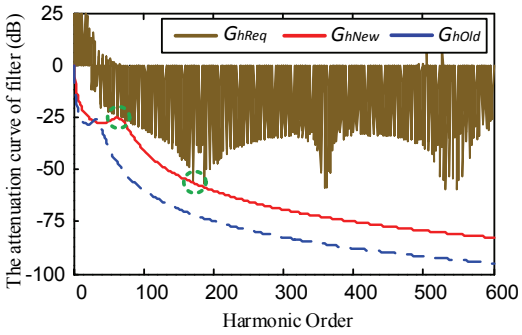

Fig. 10. Attenuation curve of LCL filter

using the traditional method are bigger than those using new method.

The required minimum attenuation rate G_{hReq}, the attenuation rate of filters G_{hOld} by the traditional method and the attenuation rate of filters G_{hNew} by the method proposed in this paper are described as corresponding curves and compared, as shown in Fig. 10.

From the attenuation curve of three-level LCL filter shown in Fig. 10, the attenuation curve of filters with the traditional method G_{hOld} shows downward deviation and is relatively far from the required minimum attenuation rate G_{hReq}. The attenuation curves of filters with the method proposed in this paper G_{hNew} is closer to G_{hReq} than G_{hOld}, and in terms of $G_{hNew}<G_{hOld}$, it can be known that the filters meet the suppression requirements of each current harmonic.

4. Experimental Verification

An experimental platform according to the system parameters given above in section 3.5 is built. The comparative analysis of two different sets of filter parameters in Table 1 for the experimental platform are made as follows.

The calculated values for harmonic spectrum of grid current with the traditional method and the method proposed in this paper are shown in Fig. 11.

To verify the results of the above design, a three-level three-phase PWM converter prototype with TMS320F 28335 as the control center is established, and the YO KOGAWA power analyzer (WT1800) is adopted to measure the harmonic spectrum of grid current. With the traditional method, the parameter L is 4.0mH@21A, L_g is 2.0mH@21A, and C_f is 6uF when Voltech transformer tester (AT3600) is used for inductance measurement under the condition of DC bias as 21A. However, with the method proposed in this paper, L is 1.6mH@21A, L_g is 1.3mH @21A and C_f is 2.2uF under the same condition. And the

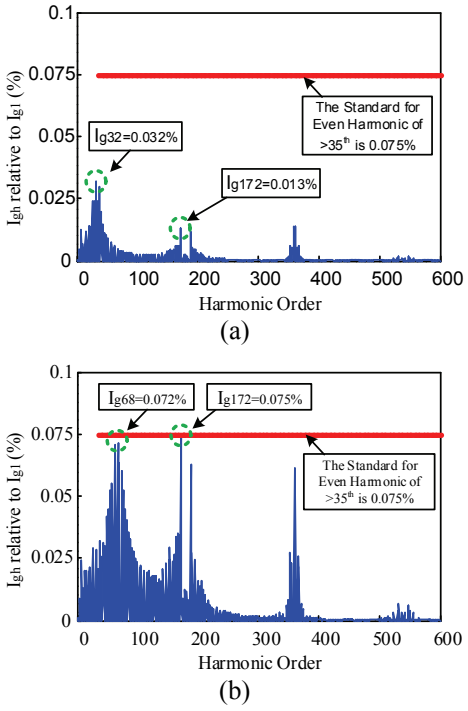

Fig. 11. Calculated value of harmonic spectrum of grid current: (a) The traditional method; (b) The method proposed in this paper

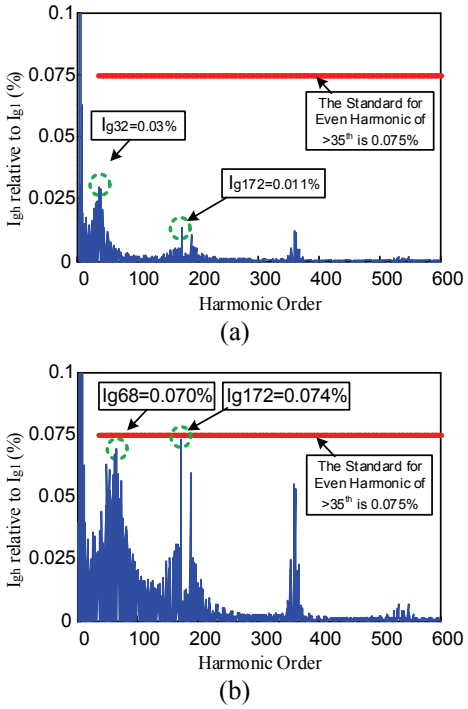

Fig. 12. Measured value of harmonic spectrum of grid current: (a) The traditional method; (b) The method proposed in this paper

measured values for harmonic spectrum of grid current is shown in Fig. 12.

From the grid current harmonics shown in Fig. 12 (a) and Fig. 12 (a), the value of each current harmonic obtained by

the traditional method is smaller, that is, its filtering effect is better, but from Table 1 it can be seen that its filter parameters are too large. Meanwhile, from Table 1 it can be seen that with the method proposed in this paper this method, the obtained value of each current harmonic is larger but can meet the requirements given by IEEE519, and the obtained filter parameters L, L_g and C_f are smaller, and the total value of inductance and capacitance value are decreased by about half.

From Fig. 12, it can be found that the current harmonic orders in the resonant frequency, the first, second and third of switching frequency and its sideband are the key points. Therefore, a comparison between the calculated value and the experimental value for grid current harmonic with the traditional method and the new method proposed in this paper are shown in Table 2.

Table 2. Contrast of current harmonic before and after LCL filter parameters optimization

Name		I_{gres}/%	I_{g172}/%	I_{g359}/%	I_{g532}/%
Traditional method	Calculated value	0.032	0.013	0.014	0.0017
	Measured value	0.030	0.011	0.011	0.0010
New method	Calculated value	0.072	0.075	0.060	0.0070
	Measured value	0.070	0.074	0.055	0.0064

From Table 2, the value of current harmonics obtained by the method proposed in this paper is closer to standard value than traditional methods, which is especially closer to the standard value of 0.075% when the frequency is resonant frequency and one time switching frequency. In addition, it can be seen from Fig. 11, Fig. 12 and Table 2 that the calculated and experimental values of grid current harmonic have high consistency at the resonance frequency f_{res} and opening frequency f_{sw}, $2f_{sw}$ and $4f_{sw}$, indicating the effectiveness of the calculation method for current harmonics proposed in this paper.

LCL filter is used to suppress high harmonics, but due to the presence of dead zone for PWM in practical application, low-order harmonics are existed in actual grid current, which are mainly composed of 5, 7, 11 and 13-order harmonics. However, harmonic compensation can be realized for the low-order harmonics by means of control, and thus the validity of this method is not affected.

5. Conclusion

In the paper, an optimization method for parameters of least square method based LCL filter is proposed. The required minimum attenuation rate is obtained by combining the calculated voltage harmonics generated by PWM and standard of each grid current harmonic. Then, with the goal of minimizing parameter values for LCL filter, a three-dimensional global search for LCL filter parameters is performed, making the actual attenuation curve approximating the required minimum attenuation rate. Based on the constraint scopes for LCL filter parameters of the traditional method, this paper searches for the optimal filter parameters by optimizing the algorithm, which has addressed the problem of the traditional method, that is, it requires repeated trial and simulation of parameters. Finally, the effectiveness of this method has verified by the experimental results.

References

[1] Xiong Jian, Kang Yong. Study of the Control Technology of Three phase Voltage Source PWM Rectifier [J]. Power Electronics, 1999, 33(2): 5-7.

[2] Wu Xiaojie Luo Yuehua Qiao Shutong. A Control Technical Summary of Three-Phase Voltage-Source PWM Rectifiers [J]. Transactions of China Electrotechnical Society, 2005, 20(12): 7-12.

[3] Pahlevaninezhad M, Das P, Drobnik J, et al. A new control approach based on the differential flatness theory for an AC/DC converter used in electric vehicles [J]. Power Electronics, IEEE Transactions on, 2012, 27(4): 2085-2103.

[4] Portillo R C, Prats M M, León J I, et al. Modeling strategy for back-to-back three-level converters applied to high-power wind turbines [J]. Industrial Electronics, IEEE Transactions on, 2006, 53(5): 1483-1491.

[5] M Liserre, F Blaabjerg, A Dell'Aquila. Step-by-step design procedure for a grid-connected three-phase PWM voltage source converter [J]. International Journal of Electronics, 2004, 91(8): 445-460.

[6] Liserre M, Blaabjerg F, Hansen S. Design and control of an LCL-filter-based three-phase active rectifier [J]. Industry Applications, IEEE Transactions on, 2005, 41(5): 1281-1291.

[7] Liu F, Zha X, Zhou Y, et al. Design and research on parameter of LCL filter in three-phase grid-connected converter[C]//Power Electronics and Motion Control Conference, 2009. IPEMC'09. IEEE 6th International. IEEE, 2009: 2174-2177.

[8] Zhang Chouwei, Zhang Xing. PWM Rectifier and Control [M]. China Machine PRESS, 2003.

[9] Ren B, Sun X, An S, et al. Analysis and design of an LCL filter for the three-level grid-connected converter [C]//Power Electronics and Motion Control Conference (IPEMC), 2012 7th International. IEEE, 2012, 3: 2023-2027.

[10] Li Xinran, Guo Xizheng, Wang Dewei, et al. Research and Development of High-power Three-Phase Voltage Source PWM Rectifier With LCL Filter [J]. Transaction of China Electrotechnical Society, 2011, 26(8): 79-84.

[11] Zheng Xinxin, Xiao Lan, Wang Changbao, et al. A New Parameter Optimization Method of LCL Filter in Three-phase Converters[J]. Proceedings of CSEE, 2013, 33(12): 55-63.

[12] Hang Yafeng, Li, Long, Yan Gangui, et al. Parameter optimization design for LCL filter of large capacity PV converter [J]. Power System Protection and Control, 2013, 41(21): 104-109.
[13] Chen Yao, Tong Yibin, Jin Xinmin. A Novel Algorithm of SVPWM Harmonic Analysis Based on PWM Rectifier [J]. Proceedings of CSEE, 2001, 21(5): 79-83.
[14] Li Qiming. Method and Simulation of Three-Level SVPWM Control Strategy [D]. Hefei University of Technology, 2007

Hong Zheng He received Master degree in control science and engineering from Sichuan University. His research interests are renewable energy system control and power electronics and motion control.

Zheng-feng Liang He received B.S degree in Automation Engineering from university of Electronic Science and Technology of China. Currently, he is a M.S student in Automation Engineering, Electronic Science and Technology University, China. His research interests are power electronics, filtering and storage converters.

Meng-shu Li She received B.S degree in Automation Engineering from University of Electronic Science and Technology of China. Currently, she is a M.S student in Automation Engineering, Electronic Science and Technology University, China. Her research interests are power electronics, filtering and storage converters.

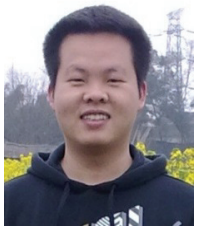

Kai Li He received his B.S, M.S and PhD degree in Automation Engineering from University of Electronic Science and Technology of China, China, in 2006, 2009 and 2014. Currently, he is a Lecturer Professor in University of Electronic Science and Technology of China. His research interests include multilevel inverters, storage converters and microgrid.

Appendix

Table 1. Duty cycle of u_{ao} in other sections

Section	Duty cycle of u_{ao}	Section	Duty cycle of u_{ao}
I1	$d^+_{u(k)} = m_u \sin(60^\circ - r)$	I2	$d^+_{u(k)} = m_u \sin(r) + 2m_u \sin(60^o - r)$
I3	$d^+_{u(k)} = 2m_u \sin(r + 60^\circ) - m_u \sin(r) - 0.5$	I4	$d^+_{u(k)} = m_u \sin(60^\circ - r) + 0.5$
I5	$d^+_{u(k)} = m_u \sin(r + 60^\circ)$	I6	$d^+_{u(k)} = m_u \sin(r + 60^\circ)$
II1	$d^+_k = m_u \sin(60^\circ - r)$	II2	$d^-_k = -m_u \sin(r)$
II3	$d^+_k = 0.5 - m_u \sin(r)$	II4	$d^-_k = -0.5 + m_u \sin(60^\circ - r)$
II5	$d^+_k = 2m_u \sin(r) - m_u \sin(60^\circ + r)$	II6	$d^-_k = -2m_u \sin(r) + m_u \sin(60^\circ + r)$
III1	$d^-_k = -m_u \sin(60^\circ - r) - 2m_u \sin(r)$	III2	$d^-_k = -m_u \sin(r)$
III3	$d^-_k = -m_u \sin(r) - 0.5$	III4	$d^-_k = -m_u \sin(r - 60^\circ) - 2m_u \sin(r) + 0.5$
III5	$d^-_k = -m_u \sin(60^\circ + r)$	III6	$d^-_k = -m_u \sin(60^o + r)$
IV1	$d^-_k = -m_u \sin(60^\circ - r)$	IV2	$d^-_k = -m_u \sin(r) - 2m_u \sin(60^o - r)$
IV3	$d^-_k = -2m_u \sin(r + 60^\circ) + m_u \sin(r) + 0.5$	IV4	$d^-_k = -m_u \sin(60^\circ - r) - 0.5$
IV5	$d^-_k = -m_u \sin(r + 60^\circ)$	IV6	$d^-_k = -m_u \sin(r + 60^\circ)$
V1	$d^-_k = -m_u \sin(60^\circ - r)$	V2	$d^+_k = m_u \sin(r)$
V3	$d^-_k = -0.5 + m_u \sin(r)$	V4	$d^+_k = -m_u \sin(r) = 0.5 - m_u \sin(60^\circ - r)$
V5	$d^-_k = -2m_u \sin(r) + m_u \sin(60^\circ + r)$	V6	$d^+_k = 2m_u \sin(r) - m_u \sin(60^\circ + r)$
VI1	$d^+_k = m_u \sin(60^\circ - r) + 2m_u \sin(r)$	VI2	$d^+_k = m_u \sin(r)$
VI3	$d^+_k = m_u \sin(r) + 0.5$	VI4	$d^+_k = m_u \sin(r - 60^\circ) + 2m_u \sin(r) - 0.5$
VI5	$d^+_k = m_u \sin(60^\circ + r)$	VI6	$d^+_k = m_u \sin(60^o + r)$